BCL2A1- and G0S2-driven neutrophil extracellular traps: A protective mechanism linking preeclampsia to reduced breast cancer risk

LU XIAO[1*], JING LI[1*], JIAHAO LIAO[2], MIN WU[1], XIUJING LU[1], JIEHUA LI[2] and YACHANG ZENG[1]

[1]Department of Obstetrics and Gynecology, The First Affiliated Hospital of Guangxi Medical University, Nanning, Guangxi Zhuang Autonomous Region 530021, P.R. China; [2]Department of Gastrointestinal Gland Surgery, The First Affiliated Hospital of Guangxi Medical University, Nanning, Guangxi Zhuang Autonomous Region 530021, P.R. China

Received December 4, 2024; Accepted March 18, 2025

DOI: 10.3892/or.2025.8897

Abstract. Preeclampsia has been associated with a reduced risk of breast cancer (BC), but the mechanisms underlying this relationship remain unclear. It has been suggested that neutrophil extracellular traps (NETs), which are released upon neutrophil activation, play a key role in both preeclampsia and BC. To investigate this link, the single-cell RNA sequencing dataset GSE173193 was analyzed and upregulated genes BCL2A1 and G0/G1 switch gene 2 (G0S2) were identified in neutrophils from preeclamptic placentas. These findings were validated using reverse transcription-quantitative PCR and western blotting. Combined analyses of preeclampsia and BC tissues, from Gene Expression Omnibus (GSE24129) and The Cancer Genome Atlas databases respectively, identified 2,040 upregulated differentially expressed genes, including BCL2A1 and G0S2. Furthermore, these genes showed clinical relevance to BC, as demonstrated by Receiver Operating Characteristic curve, survival analyses and weighted gene co-expression network analysis. Functional experiments revealed that overexpression of BCL2A1 and G0S2 increased NET release and inhibited BC cell proliferation, invasion and migration. The present study provides novel insights into the shared molecular pathways of preeclampsia and BC, emphasizing NETs as a potential protective mechanism as increased NET production in preeclampsia may contribute to a reduced BC risk by influencing tumor progression and offer avenues for further research into therapeutic interventions.

Correspondence to: Professor Jiehua Li, Department of Gastrointestinal Gland Surgery, The First Affiliated Hospital of Guangxi Medical University, 6 Shuangyong Road, Nanning, Guangxi Zhuang Autonomous Region 530021, P.R. China
E-mail: lijiehua01@sina.com

Professor Yachang Zeng, Department of Obstetrics and Gynecology, The First Affiliated Hospital of Guangxi Medical University, 6 Shuangyong Road, Nanning, Guangxi Zhuang Autonomous Region 530021, P.R. China
E-mail: 420300@sr.gxmu.edu.cn

*Contributed equally

Abbreviations: CCK-8, Cell Counting Kit-8; DEGs, differentially expressed genes; G0S2, G0/G1 switch gene 2; GO, Gene Ontology; KEGG, Kyoto Encyclopedia of Genes and Genomes; NETs, neutrophil extracellular traps; NF-κB, nuclear factor κB; PCA, principal component analysis; PRRs, pattern recognition receptors; RT-qPCR, reverse transcription-quantitative PCR; ROS, reactive oxygen species; scRNA-seq, single-cell RNA sequencing; TANs, tumor-associated neutrophils; UMAP, Uniform Manifold Approximation and Projection; WGCNA, weighted gene co-expression network analysis

Key words: preeclampsia, breast cancer, BCL2A1, G0S2, neutrophils, NETs

Introduction

Preeclampsia is a pregnancy-specific disease associated with obstruction of uterine spiral arteries, excessive activation of inflammatory immunity, endothelial cell damage, genetic factors, metabolic dysfunction and nutritional deficiencies (1-3). In total, ~4 million women are diagnosed with preeclampsia annually worldwide, leading to over 70,000 maternal and 500,000 infant deaths (4). The prognosis of preeclampsia remains elusive, particularly in late onset cases. SPARC plays a crucial role in placenta development, and its downregulation under hypoxic conditions potentially contributes to preeclampsia and -associated intrauterine growth restriction (5). Similarly, maternal microRNA-125b plasma levels in the first trimester have been shown to strongly predict pre-eclampsia way before clinical manifestations (6). Women with a history of pre-eclampsia have approximately double the risk of cardiovascular disease, including cardiovascular-related death, coronary artery disease, heart failure and stroke, persisting for up to 39 years of follow-up (7). According to global cancer statistics for 2020, breast cancer (BC) is the most common malignant tumor worldwide, posing serious risks to women's physical and mental health (8). The epidemiological link between preeclampsia and BC was first described in a 1983 case-control study by Polednak and Janerich, which

showed reduced BC risk before age 45 among women with preeclampsia during their first pregnancy (9). Subsequent studies over the past 40 years have provided increasing evidence of this association.

Neutrophils, the most abundant immune cells, have been identified to play a significant role in preeclampsia. In preeclamptic patients, neutrophils are heavily activated, increasing superoxide production, systemic inflammation and vascular endothelial damage (10). Activated neutrophils interact with platelets through signaling pathways involving chemokines and adhesion factors, contributing to preeclampsia development (11). Platelet-activating factor released by platelets also plays a key role in the condition's pathogenesis (12). Previous studies revealed that neutrophils accelerate endothelial cell apoptosis through increased NET expression, a critical step in vascular endothelial injury in preeclampsia (13). In tumors, neutrophils, known as tumor-associated neutrophils (TANs), are a heterogeneous and integral component of the tumor microenvironment, with dual roles in tumor promotion and prevention (14,15). Fridlender *et al* (16) in 2009 introduced the N1 (antitumor) and N2 (protumor) nomenclature for TANs. Neutrophils can mediate cytotoxicity against tumor cells via reactive oxygen species (ROS) such as hydrogen peroxide and superoxide, with ROS-mediated elimination depending on TRPM2, an H_2O_2-dependent Ca^{2+} channel (17). Neutrophils can also present antigens to T cells, inducing IFN-γ production and adaptive immune responses, or directly interact with T cells to lower activation thresholds, aiding tumor cell clearance (18,19). These findings suggest that NETs produced by neutrophils may provide a crucial link between preeclampsia and reduced BC risk.

In recent years, integrative genomic analyses have advanced the understanding of shared pathogenesis between diseases. The present study employed single-cell sequencing and bioinformatics to investigate the relationship between neutrophils and the reduced risk of BC in preeclamptic patients. Supported by *in vitro* validation, the findings suggest that NETs mediate a protective mechanism linking preeclampsia to a reduced risk of BC. The pivotal roles of BCL2A1 and G0/G1 switch gene 2 (G0S2) in regulating neutrophil activity and NET production underscore their potential as therapeutic targets for cancer and inflammatory diseases.

Materials and methods

Reagents and kits. List of reagents and kits used in the study are provided along with company names and cat. nos. in Table SI.

Data sources. A scRNA-seq dataset (GSE173193) was obtained from Gene Expression Omnibus (GEO) database (https://www.ncbi.nlm.nih.gov/geo/). This dataset contained placental tissue samples of the gestational diabetes group (n=2), preeclampsia group (n=2), advanced age group (n=2) and normal control group (n=2). Normal control group (n=2) and preeclampsia group (n=2) were used to characterize cellular landscape of preeclampsia.

Single cell sequencing data analysis processing

Quality control. Initially, the DropletUtils package (20) was utilized to assess the expression levels of each cell and to filter out barcoded cells that showed no expression. Next, cells were further filtered based on their unique molecular identifier counts. Subsequently, the scatter package (21) was employed to quantify gene expression in the cells, leading to the exclusion of cells with mitochondrial gene proportions >10% and ribosomal gene proportions <10%. Finally, gene counts were obtained.

Data preprocessing and principal component analysis (PCA). First, the NormalizeData function from the Seurat package (22) was employed to standardize the expression matrix of the filtered samples. Next, the FindVariableFeatures function was used to identify the first 2,000 genes with the most significant differences among cells. Concentrating on these genes in subsequent analyses will enhance the detection of biological signals in single-cell datasets. Following this, the expression data were linearly scaled using the ScaleData function from the Seurat package. Finally, PCA was conducted using the RunPCA function within the Seurat package.

Cell cluster and annotation. First, principal components with high standard deviations were selected. Next, cell clustering analysis was conducted using the FindNeighbors and FindClusters functions from the Seurat package. Then, Uniform Manifold Approximation and Projection (UMAP) for dimensionality reduction was performed using the RunUMAP function of the Seurat package. Cell types were annotated based on the known marker genes.

Identification of marker genes. To identify differentially expressed genes (DEGs) between each cluster and all other cells, the FindAllMarkers function from the Seurat package was utilized. Novel marker genes were determined based on the following criteria: (log2FC ≥0.1, a minimum expression ratio of cell population=0.25, and P≤0.05), resulting in the selection of the top 500 logFC markers (23). Cells were then labeled according to the known marker genes, and a cluster display diagram was created.

Cell-cell communication analysis. CellChatv1.1 (24) was used to infer the communication between cells according to the corresponding receptor ligand gene expression values of various cells. And then, the receptor ligand pair network between cells was obtained.

Pseudotime analysis. Pseudotime analysis was conducted using Monocle (25). First, genes expressed in at least 5% of the cells were selected. Next, the reduceDimension function was applied to perform dimensionality reduction analysis, followed by clustering of the cells using the clusterCells function. The differentialGeneTest function was then used to identify candidate genes that differed between the clusters with a P<0.05. Dimensionality reduction analysis of the cells was performed using the DDRTree method and the reduceDimension function based on the candidate genes. Finally, the orderCells function was utilized to arrange and visualize the cells along a quasi-chronological trajectory.

DEG analysis and functional enrichment analysis. DEGs were identified using the FindMarkers function (test.use=MAST) in Seurat. A P<0.05 and a log2 fold change >0.58 were established as the criteria for significant differential expression. Gene Ontology (GO) enrichment and KEGG pathway enrichment analyses of the DEGs were performed using the DAVID

database, (https://davidbioinformatics.nih.gov/) encompassing all GO categories, including biological processes, cellular components and molecular functions.

Identification of significant DEGs in preeclampsia and BC. The 'limma' function from the R suite was employed to identify DEGs from The Cancer Genome Atlas-BC and GSE24129 datasets. DEGs were classified as those exhibiting |log2 (fold change)|>1 and P<0.01. The findings are presented using volcano plots.

Construction and visualization of the co-expression network. The DEGs were analyzed for co-expression networks using the R package Weighted Gene Co-expression Network Analysis (WGCNA) (26). WGCNA was employed to construct a gene co-expression network based on the standardized gene data in order to identify the optimal soft threshold. A scale-free network was built using this best soft threshold, and the genes were then clustered into functional modules, each represented by different colors, with clustering and classification performed using the dynamic tree cutting algorithm. Finally, PCA was applied to describe the module eigengenes, which reflect a unique expression profile for all the genes within each module. The correlations between these eigengenes and clinical characteristics were calculated to determine which modules were clinically relevant.

Patient samples. In the present study, the inclusion criteria for patients with BC included a preoperative diagnosis confirmed by Mammotome biopsy and no prior history of radiation therapy or chemotherapy. Tumor tissue samples, along with adjacent normal tissues (control), were collected from 3 patients with BC, aged 40 to 70 years, with a median age of 55. The inclusion criteria for patients with preeclampsia required a clear clinical diagnosis, absence of other complications and a singleton cesarean delivery. A total of 3 placenta samples were collected from both patients with preeclampsia and control subjects, aged 20-40 years, with a median age of 29 in the preeclampsia group and 32 in the control group. Written informed consent was obtained from all study participants for the use of tissue samples in scientific research. The present study was conducted in accordance with the ethical guidelines and was approved (approval no. 2022-E0118) by the Ethical Review Committee of the First Affiliated Hospital of Guangxi Medical University (Nanning, China).

Flow cytometric analysis. The cells obtained from freshly excised preeclampsia and control tissues were washed and centrifuged (300 x g, 4˚C, 5 min), after which a dye was added, and the cells were incubated in the dark for 30 min before being promptly quantified using flow cytometry. The detection reagents used were FITC-conjugated anti-GR-1 (cat. no. 65140-1-Ig; Proteintech Group, Inc.) and PE-Cy5-conjugated anti-F4/80 (cat. no. B281020; BioLegend, Inc.). Fluorochrome labeling: GR-1: FITC (detected in FL1 channel) and F4/80: PE-Cy5 (detected in FL3 channel). BD FACSVerse flow cytometer (Becton Dickinson) was used, and data analysis was conducted using FlowJo software (version 10; Tree Star, Inc.).

RNA extraction and reverse transcription-quantitative PCR (RT-qPCR). Total RNA was extracted from preeclampsia and BC samples using TRIzol® reagent and cDNA was synthesized with the TRUEscript H Minus M-MuLV Reverse Transcriptase. Enzymes and reagents used included: Reverse transcriptase (TRUEscript H Minus M-MuLV; cat. no. PC1703; Aidlab), RNase inhibitor (RNasin; cat. no. RN3501; Aidlab) and nucleotides (dNTP Mixture; 10 mM each; cat. no. PC2403; Aidlab). All primers were designed using Primer Premier 5.0 software (https://primer-premier.software.informer.com/) and were commercially synthesized by Sangon Biotech Co., Ltd. GAPDH was used as an internal control. The cDNA was stored at -20˚C until needed. The reverse transcription protocol was performed as follows: 42˚C for 60 min followed by 70˚C for 10 min. A two-step RT-qPCR was conducted with SYBR Green Master Mix (cat. no. PC3302; Aidlab) to assess the expression levels of BCL2A1 and G0S2. Thermocycling conditions were as follows: Initial denaturation at 94˚C for 10 min; followed 40 cycles of denaturation at 94˚C for 20 sec, annealing at 55˚C for 20 sec and extension at 72˚C for 20 sec. The primers used in the present study are listed in Table SII. GAPDH was used as housekeeping control. Data were calculated using the $2^{-\Delta\Delta Cq}$ method (27).

Western blot analysis. Total proteins were extracted from cells lysed in RIPA buffer (cat. no. P0013B; Beyotime Institute of Biotechnology). Next, the concentration of proteins was detected by BCA analysis. The extracted proteins were collected, denatured and separated using 10% SDS-PAGE gels. The samples (30 μg) were loaded onto the gels, and electrophoresis was conducted for 120 min. Following this, the proteins were transferred to PVDF membranes and blocked with 5% skimmed milk by incubation at 37˚C for 2 h. After shaking for 1 h, elution was performed. Next, the membranes were incubated with primary antibodies (Table SIII) at 4˚C overnight with shaking. Next day, the PVDF membrane was washed with TBST (0.1% Tween-20) and subjected to secondary antibody (Table SIII) incubation for 1 h at room temperature (RT). The images were acquired using the Infrared electrochemical luminescence (cat. no. ECL-0011; Beijing Dingguo Changsheng Biotechnology Co., Ltd.). The gray value of the target bands was calculated using ImageJ software 2.0 (National institutes of Health). The experiment was repeated 3 times. The housekeeping gene β-actin was used as loading control.

Immunofluorescence staining. After rehydration through graded ethanol (100→70%), tissue sections were washed with PBS and underwent antigen retrieval (cat. no. P0086; Beyotime Institute of Biotechnology) via microwave heating in retrieval buffer at low power for 15 min. Following PBS washes, sections were permeabilized with 0.1% Triton X-100 for 10 min at RT and blocked with 5% BSA at 37˚C for 1 h. Primary antibodies (anti-BCL2A1 and anti-G0S2; diluted at 1:10,000-1:40,000) were incubated at 37˚C for 2 h, followed by 3x5 min PBS washes. Fluorescent secondary antibodies, including Cy3-labeled anti-rabbit (cat. no. SA00009-2) and FITC-labeled anti-mouse (cat. no. SA00003-1; both from Proteintech Group, Inc.), were incubated at 37˚C for 1 h. After nuclear staining with Hoechst (cat. no. P0133;

Beyotime Institute of Biotechnology) at RT for 15 min and final PBS washes, slides were dehydrated in absolute ethanol for 1 min, air-dried, and mounted with antifade medium (cat. no. P0128M; Beyotime Institute of Biotechnology). Images were acquired using an inverted confocal microscope (IX71; Olympus Corporation).

Cell culture and transfection. Cells were used to identify neutrophils, which were subsequently cultured in RPMI-1640 (cat. no. 12633020; Gibco; Thermo Fisher Scientific, Inc.) medium supplemented with 10% FBS + 1% penicillin-streptomycin at 37˚C and 5% CO_2. Cells with favorable proliferation status were transfected with 50 nM small interfering RNA (siRNA). Cells were seeded in six-well plates at a density of $5x10^5$ cells per well and cultured until reaching 80% confluency. Transfection was then performed using Lipofectamine 3000 (Thermo Fisher Scientific, Inc.), followed by 6 h incubation at 37˚C with 5% CO_2 before medium change Neutrophils were divided into 5 groups: Control, vector, BCL2A1-OE, G0S2-OE and BCL2A1-OE + G0S2-OE. Neutrophils and MCF-7 cells ($5x10^5$ cells/ml) were separately seeded in a two-chamber culture system. Using a Transwell model, MCF-7 cells were plated in the lower chamber with culture medium in the upper chamber. Neutrophils ($1x10^6$ cells/ml) were then seeded in the upper compartment of the Transwell insert and co-cultured with the lower-chamber breast cancer cells for 24 h under standard incubation conditions. MCF-7 cells (cat. no. HTB-22) were purchased from the American Type Culture Collection.

Cell Counting Kit-8 (CCK-8) assays. Assays were conducted using a CCK-8 reagent. The cells were plated in 96-well plates at a density of $1x10^4$ cells per well. Next, 10 μl of CCK-8 was added to each well in a light-protected environment. The cells were then incubated at 37˚C in a 5% CO_2 atmosphere for 1.5 h. Finally, absorbance was measured at 450 nm using a ThermoMax microplate reader.

Transwell migration assay. For the cell migration assay, 200 μl of cell suspension ($1x10^5$ cells) was added to the upper compartment of a Transwell chamber with an 8-μm pore size and a 24-well insert. In each well, 50 μl of serum-free medium supplemented with 10 g/l BSA was mixed with the co-cultured cells in the upper chamber. The lower chambers contained 10% FBS. Cell migration ability was assessed by counting the number of cells that migrated to the lower chamber of the Transwell using a fluorescence microscope (IX51; Olympus Corporation).

Cell scratch assay. A total of ~$5x10^5$ cells were placed into a six-well plate, with three replicate wells designated for each group. Cells were maintained in serum-free medium throughout the assay. Once the cells adhered to the surface in a single layer, a 200-μl pipette tip was employed to create vertical scratches in the six-well plate. The cells were then washed three times with PBS, and the suspension was discarded before incubating the cells in a chamber with 5% CO_2 at 37˚C. Images were captured under a microscope at 0 and 48 h, and the experiment was repeated three times.

Statistical analysis. All statistical analyses were conducted using GraphPad Prism 8 (version 8.0; Dotmatics) and R software (version 4.2) (https://cran.r-project.org/bin/windows/base/old/4.2.0/). The data are presented as the mean ± standard deviations (SDs). Statistical analyses were performed using unpaired two-tailed t-test for two groups or one-way ANOVA for more than two groups, followed by Tukey's post hoc test for multiple comparisons. $P<0.05$ was considered to indicate a statistically significant difference.

Results

Single-cell RNA sequencing (scRNA-seq) reveals the cell composition of preeclamptic and control placentas. To examine cell-type-specific changes in preeclampsia at the single-cell level, scRNA-seq) was performed on the GSE173193 dataset, which included two control patients and two preeclamptic patients. After conducting quality control and normalization, the first 2,000 highly variable genes within the cells were identified (Fig. 1A). Dimensionality reduction was then performed using PCA to analyze the linearly scaled scRNA data, focusing on the top two principal components for further investigation. The PCA results indicated a distinct separation between preeclamptic and control placental cells (Fig. 1B). Based on the elbow point criterion, the optimal number of principal components was determined to be 10 (Fig. 1C). Heatmaps illustrating the top 20 marker genes for each principal component are shown (Fig. 1D). Using the UMAP method, the placental cells were clustered into 18 groups (Fig. 1E). The top ten marker genes of each cell cluster are presented in Figs. S1 (group 0-8) and S2 (group 9-17).

Identification of cell types and their marker genes in placental cells. Next it was aimed to identify various cell types within placental cells from both normal individuals and patients with preeclampsia. Using known marker genes, 12 distinct cell types were annotated (Fig. 2A). The relative abundance of each cell type is illustrated in Fig. 2B. Notably, differences in the ratios of placental cells were observed between preeclampsia patients and controls. By applying a $|\log FC| \geq 0.1$, a minimum expression ratio of the cell population of 0.25, and a $P \leq 0.05$, novel marker genes were identified for each cell type. The top ten marker genes for each cell type were visualized as follows: Neutrophils (ALOX5AP, BCL2A1, CAMP, CXCL8, G0S2, IFITM2, RETN, S100A12, S100A8 and S100A9); villous cytotrophoblast cells (CCNB1, CDK1, HIST1H4C, HMGB1, PTTG1, STMN1, TUBA1B, TUBB, TYMS and UBE2C); extravillous trophoblast cells (AOC1, EBI3, FN1, FSTL3, HPGD, NOTUM, PAPPA2, PRG2, SERPINE2 and TAC3); and syncytio-trophoblast cells (CGA, CYP19A1, ERVFRD-1, GADD45G, GDF15, HOPX, INSL4, KISS1, KRT23 and CSH1) (Fig. S3). Additionally, the expression levels of the known marker genes used for cell type annotation were analyzed (Fig. 2C).

Cell-cell interactions based on ligand-receptor interactions and reconstruction of the temporal dynamics of trophoblasts. The placenta is formed through a complex process that requires the collaborative efforts of various cell lineages. Intercellular communications among different cell types govern the proper

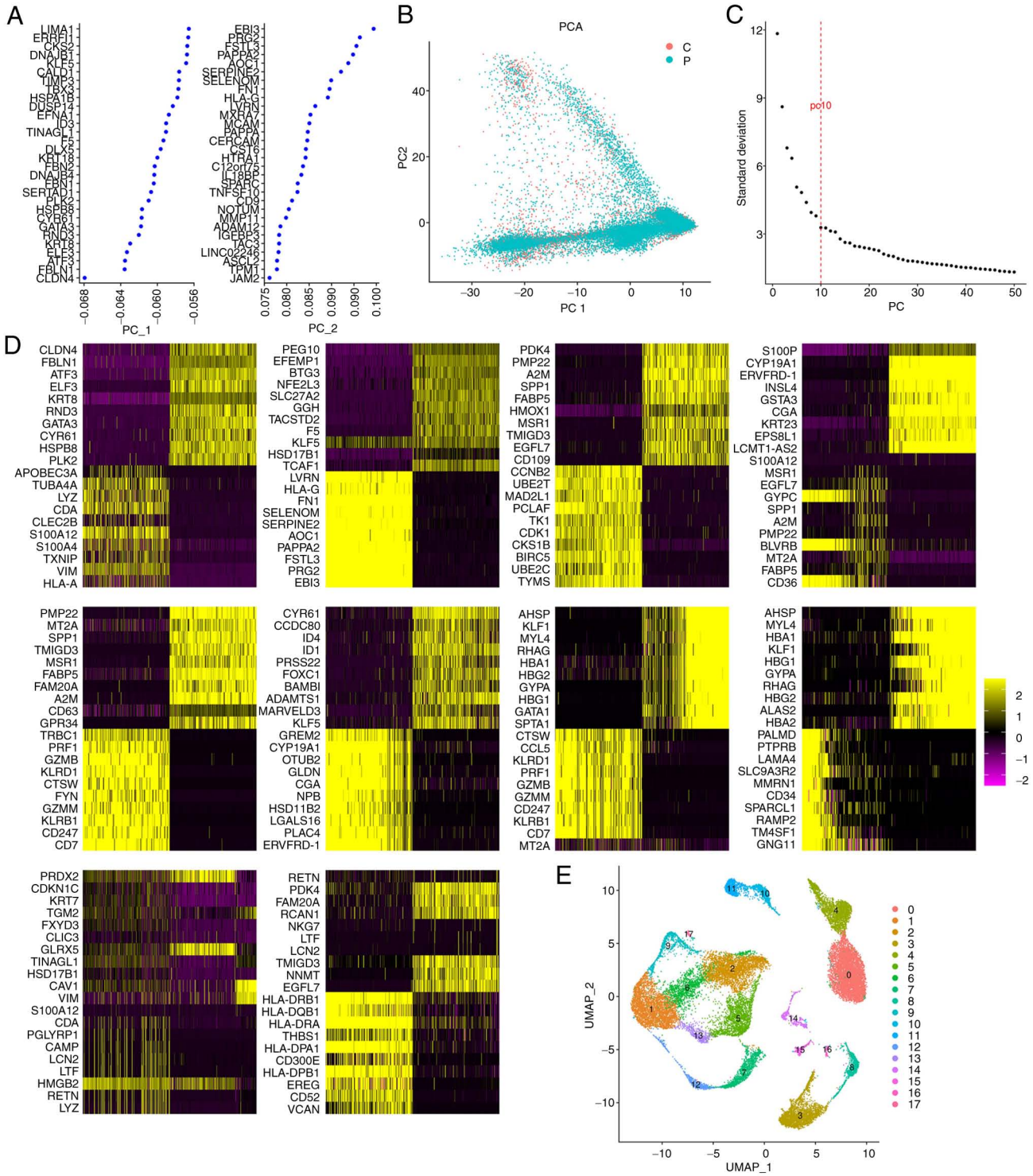

Figure 1. Cellular composition of preeclamptic and control placentas. (A) Top two principal component analyses according to standard deviation. (B) PCA plots of placenta cells between preeclampsia and control. (C) Elbow-plot determining the optimal principal components. (D) Heatmaps showing the top 20 marker genes in each principal component analysis. (E) Cell clusters based on the screened principal component analyses. PCA, principal component analysis.

functions of metazoans and heavily depend on the interactions between secreted ligands and cell-surface receptors. Based on marker genes, ligand-receptor interactions were identified. It was demonstrated that each cell type possesses a significant number of receptor ligands (Fig. 3A and B). Among these interactions, those occurring between macrophages and other cells show the highest number and intensity in the placentas of patients with preeclampsia. Additionally, there are numerous interactions between neutrophils and other cells that are characterized by high intensity as well. Overall, the present findings suggest that complex intercellular communication occurs within the placental microenvironment, with distinct changes in this communication. Furthermore, to explore the evolutionary processes of trophoblasts, the present study utilized the Monocle tool to uncover pseudo-temporal ordering due to the similarity of cell clusters with developmental lineages.

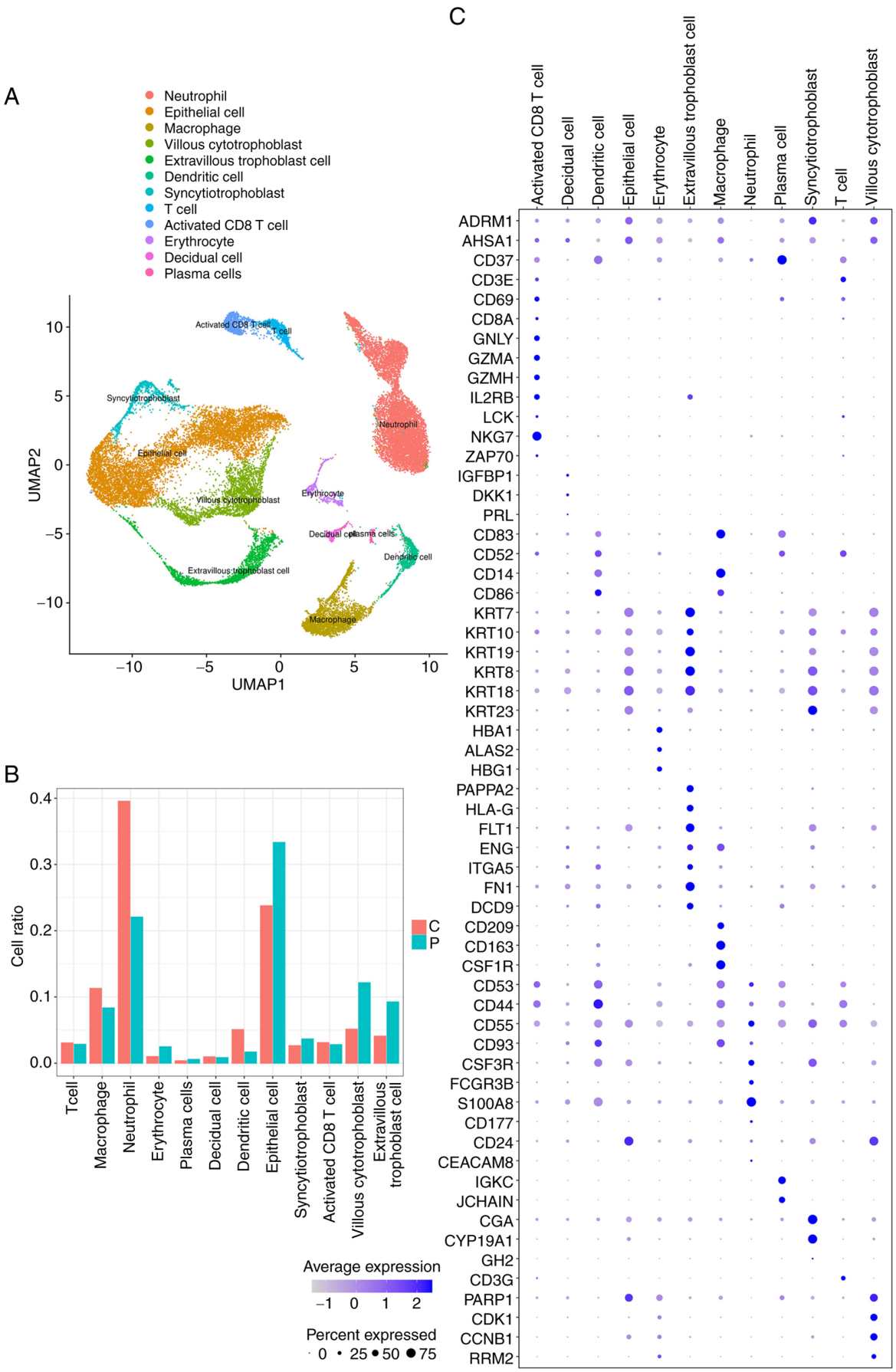

Figure 2. Identification of cell types and their marker genes across preeclampsia and control placentas cells. (A) UMAP plots showing cell types identified by marker genes. Each cell type was colored by a unique color. (B) The cell ratio among preeclampsia and control placenta cells. (C) Integrated analysis showing marker genes across cell types. The size of each circle reflects the percentage of cells in each cell type where the gene was detected, and the color shadow reflects the average expression level within each cell type. UMAP, Uniform Manifold Approximation and Projection.

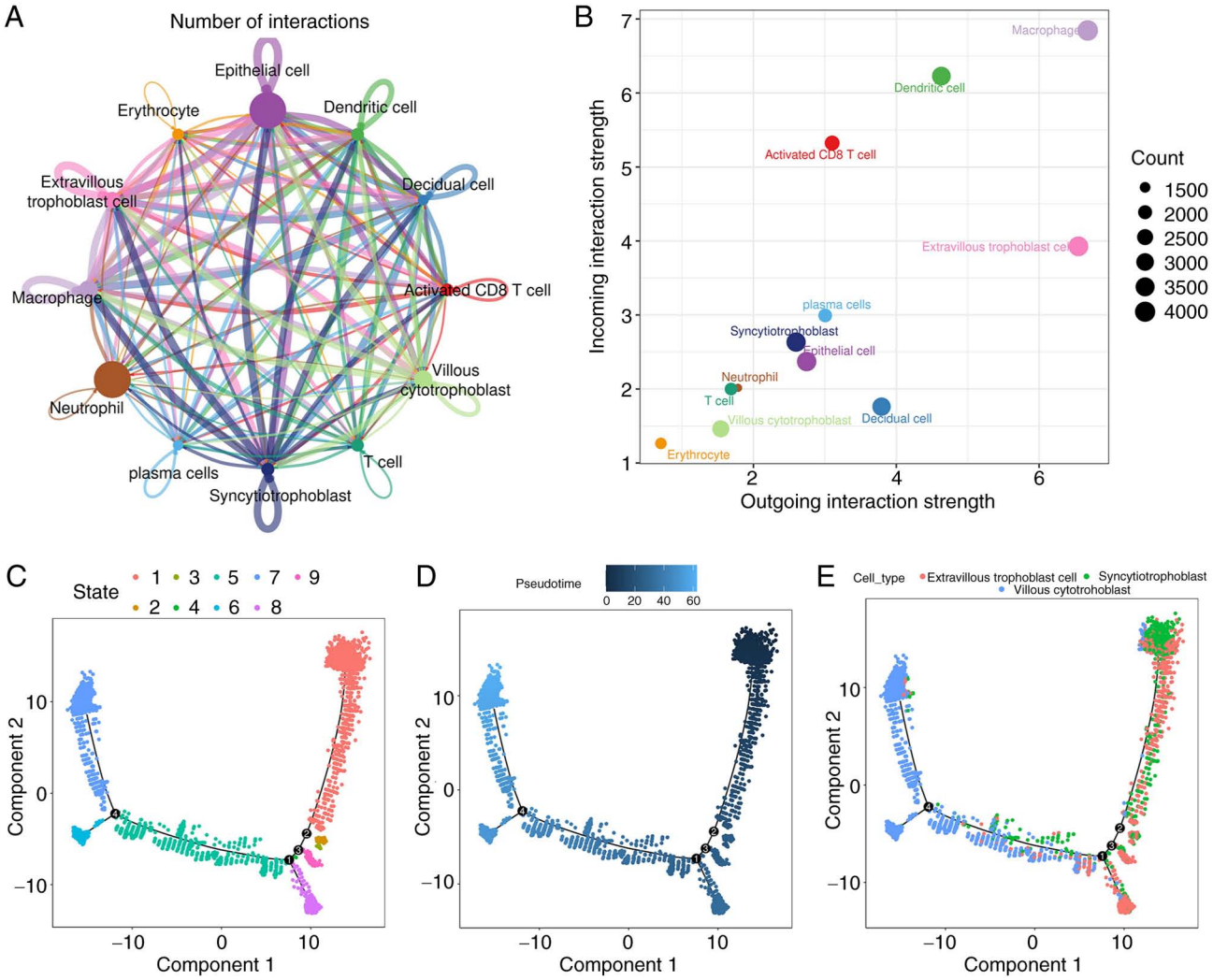

Figure 3. Intercellular communication network. (A) The solid circles with different colors represent different cell groups. The size of the solid circle is proportional to the number of cells corresponding to the cell group. The color of each side is consistent with the signal sender, and the thickness of the side is proportional to the communication intensity. (B) The color of the dot indicates different cell groups, and the size of the dot is proportional to the number of ligands and receptors inferred from each cell group. The x axis and y axis respectively indicate the strength of the cell group as a signal sender and receiver. The color of each dot represents distinct cell groups, and the size of the dot corresponds to the number of ligands and receptors inferred from each group. The x-axis and y-axis indicate the strength of the cell group as a signal sender and receiver, respectively. (C-E) Pseudotime ordering of trophocyte. Each dot represented one cell, and each branch represented one cell state. The left plot was labeled with cell states, and the right plot was labeled with developmental time; each dot represented an individual cell, while each branch indicated a specific cell state. The left plot was labeled with cell states, whereas the right plot was labeled with developmental time.

The trends of pseudotime-dependent genes along the pseudotimeline were categorized into nine cell clusters of trophoblasts, each exhibiting diverse expression dynamics. The analysis indicated a progressive development of trophoblasts from Cluster 7 to Cluster 9 (Fig. 3C-E); syncytio-trophoblast and extravillous trophoblast cells were positioned at the beginning of the differentiation process, while villous cytotrophoblast cells were found at the end. This suggests that extravillous trophoblast cells or syncytio-trophoblast cells may differentiate into villous cytotrophoblast cells during the development of preeclamptic placentas, suggesting that different trophoblast subtypes may fulfill distinct biological functions.

Biological processes associated with marker genes of trophoblast and neutrophil subsets. To further investigate the functional status and potential regulatory factors associated with trophoblast and neutrophil subsets in preeclamptic placentas, GO and Kyoto Encyclopedia of Genes and Genomes (KEGG) enrichment analyses on the DEGs identified in the cell populations (Fig. 4A-D) were performed in the present study. The results indicated that in the annotated villous cytotrophoblast cell populations, the biological functions were primarily enriched in the regulation of cell metabolism, biosynthesis, mitosis and cell cycle processes. This aligns with the findings of Zhou *et al* (28). In the annotated extravillous trophoblast cell population, biological functions were mainly related to proteolysis, cell migration and movement, angiogenesis and regulation. For the annotated syncytio-trophoblast cell population, genes linked to biological functions were enriched in the positive regulation of cell apoptosis and death, as well as hormone regulation. In the annotated neutrophil population, biological functions predominantly involved cell activation, responses to cytokine stimulation, cell migration,

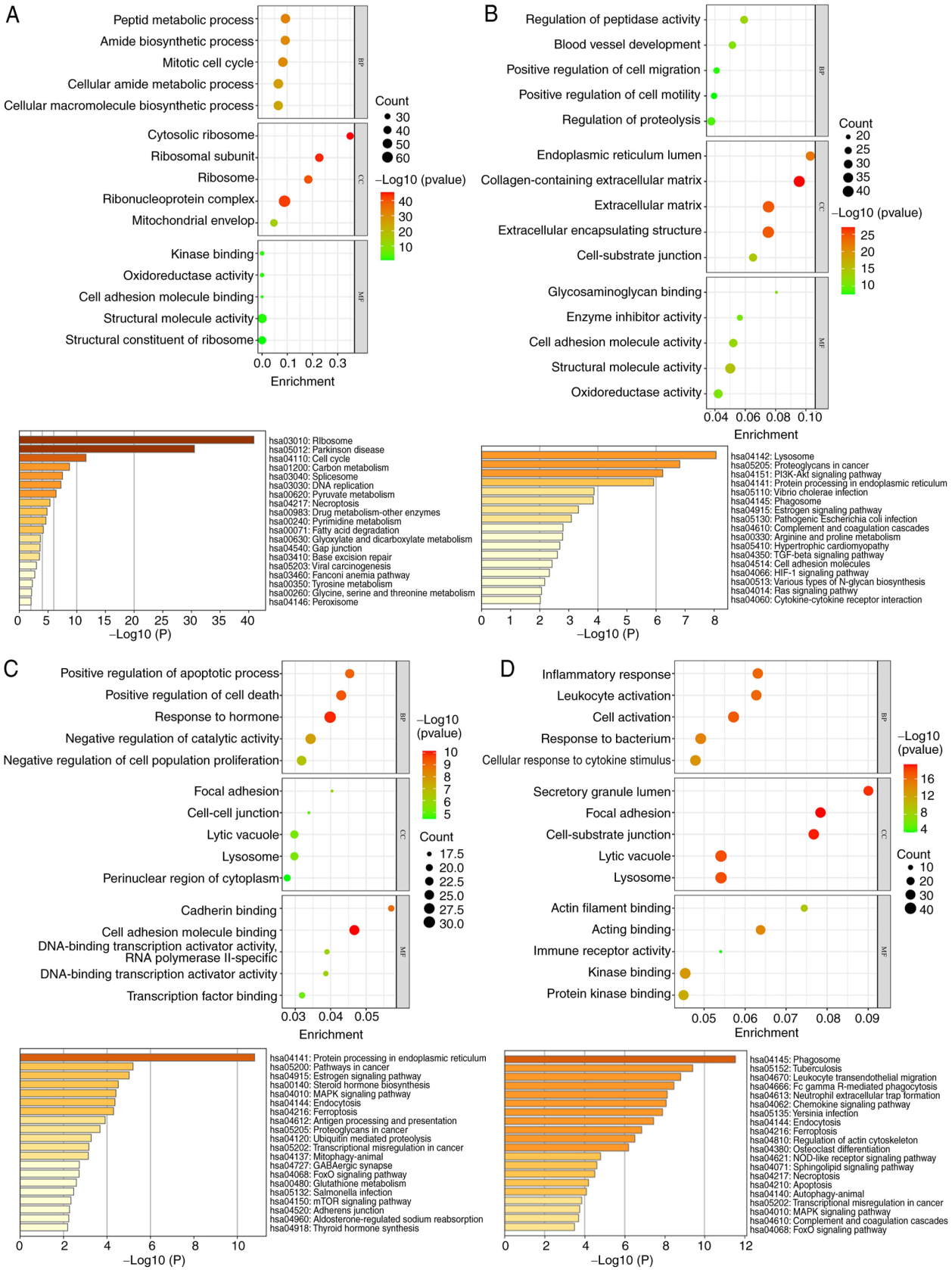

Figure 4. GO and KEGG enrichment. (A-D) GO and KEGG enrichment analysis of genes enriched in (A-C) trophoblasts and (D) neutrophils. GO, Gene Ontology; KEGG, Kyoto Encyclopedia of Genes and Genomes.

movement, the actin filament process and the inflammatory response. Regarding cell components, the genes were mainly enriched in lysosomes and secretory granules. In terms of molecular function, the genes showed enrichment primarily in kinase and protein kinase binding, actin binding, and immune receptor activity. The KEGG pathway enrichment

analysis revealed significant pathways such as phagosomes, pulmonary tuberculosis, leukocyte migration across the endothelium, Fcγ receptor-mediated phagocytosis and the formation of neutrophil extracellular traps.

BCL2A1 and G0S2 genes are significantly increased in neutrophils from preeclamptic placental tissue. The flow cytometric results indicated that GR-1 was downregulated in the preeclampsia group compared with the normal group (P<0.05; Fig. 5A). RT-qPCR results revealed that BCL2A1 and G0S2 were upregulated in the preeclampsia group relative to the normal group (P<0.05; Fig. 5B). Western blot analysis revealed that the expression of BCL2A1 and G0S2 was increased in the preeclampsia group compared with the control group (P<0.05; Fig. 5C). Immunofluorescence results demonstrated that the expression levels of BCL2A1 and G0S2 were significantly higher in the preeclampsia group than in the control group, while GR-1 expression was significantly lower in the preeclampsia group (P<0.05; Fig. 5D and E).

Overexpression of the BCL2A1 and G0S2 genes in neutrophils promotes the production of NETs. The RT-qPCR results indicated that circulating free DNA expression was upregulated in the groups overexpressing BCL2A1 and G0S2 compared with the blank group (P<0.05; Fig. 6A-C). Western blot analysis showed that the expression of PAD4, citH3, NE and MPO was increased in the BCL2A1-overexpressing and G0S2-overexpressing groups relative to the blank group (P<0.05; Fig. 6D-H).

Clinical relationship between BCL2A1 and G0S2 genes and BC. The combined analysis of the GEO (GSE24129) and TCGA-BC datasets identified 4,183 DEGs, comprising 2,040 upregulated genes and 2,143 downregulated genes (Fig. 7A). The present study specifically focused on the upregulated genes BCL2A1 and G0S2. Using the TCGA-BC database, patients were categorized into high- and low-BCL2A1 groups. To assess the diagnostic accuracy of the prognostic risk model, the areas under the time-dependent ROC curves (AUCs) were calculated. The AUCs for the risk model in predicting 3-, 5-, and 7-year survival were 0.416, 0.386, and 0.410, respectively (Fig. 7B). Additionally, patients with high BCL2A1 expression did not show significantly different overall survival (OS) compared with those with low BCL2A1 expression (Fig. 7C). In the subgroup analyses based on G0S2 expression, the AUC of the risk model for predicting 3-, 5-, and 7-year survival was 0.448, 0.426, and 0.436, respectively (Fig. 7D). Patients with high G0S2 expression also did not exhibit significantly different OS when compared with those with low G0S2 expression (Fig. 7E). These results indicated that the models lack strong predictive power. Consequently, further analysis of the DEGs between patients with preeclampsia and BC was performed using Venn diagrams, which revealed 27 overlapping upregulated DEGs, including BCL2A1 and G0S2 (Fig. 7F).

Co-expression modules for 27 DEGs. To further investigate these 27 DEGs, WGCNA was conducted to uncover the interactions and coregulatory mechanisms among them. A cluster tree of samples was constructed using a scale-free network and topological overlap based on dynamic hybrid cutting (Fig. 7G). The optimal soft threshold was determined according to the fitting index and the average degree of network connection, in line with the scale-free topology criterion (Fig. 7H). Based on this optimal soft threshold, the gene modules were categorized into two distinct modules, and a module cluster graph was created (Fig. 7I). A correlation analysis was performed between the modules and clinical features, presenting the results in a heatmap (Fig. 7J). The analysis revealed that the turquoise module exhibited the strongest correlation with tumors (R=0.77, P=5e-241; Fig. 7K). The genes within this module were then analyzed and the core genes closely associated with preeclampsia and BC (BCL2A1 and G0S2) were further identified (Fig. 7L).

Overexpression of the BCL2A1 and G0S2 genes in neutrophils inhibits malignant progression of BC cells. To validate this hypothesis, neutrophils that were overexpressing BCL2A1 and G0S2 were co-cultured with MCF-7 cells indirectly, followed by functional analysis. The results from the CCK-8 assay indicated that the combination of BCL2A1-OE and G0S2-OE led to a reduced proliferation capacity in MCF-7 cells (P<0.05; Fig. 8A). Transwell experiments demonstrated that the BCL2A1-OE + G0S2-OE group showed a significant reduction in the invasive ability of MCF-7 cells (P<0.05; Fig. 8B and C). Additionally, this group also displayed the lowest level of migration (P<0.05; Fig. 8D and E). These findings suggest that the co-culture of BC cells with neutrophils overexpressing BCL2A1 and G0S2 inhibits the proliferation, invasion and migration of BC cells.

BCL2A1 and G0S2 gene expression levels were significantly elevated in neutrophils from BC tissue, and there was also an increase in NETs. To confirm the present findings, the expression levels of BCL2A1, G0S2, cf.-DNA, PAD4, citH3, NE and MPO in BC neutrophils were assessed using RT-qPCR and western blotting. Additionally, immunofluorescence was employed to further validate the expression of the BCL2A1 and G0S2 genes in neutrophils. Notably, the RT-qPCR results indicated that the mRNA expression levels of BCL2A1 and G0S2 were significantly elevated in BC neutrophils compared with those in the control group (P<0.05; Fig. 9A). Furthermore, western blot analysis confirmed that the levels of BCL2A1, G0S2, PAD4, citH3, NE and MPO were upregulated in the BC neutrophil group compared with the blank group (P<0.05; Fig. 9B). The immunofluorescence results demonstrated that the expression of BCL2A1 and G0S2 was significantly higher in the BC tissue than in the control group, while GR-1 expression was significantly lower in the BC tissue (P<0.05; Fig. 9C and D). Collectively, these data suggest that the BCL2A1 and G0S2 genes play essential roles in regulating neutrophil survival in BC tissues.

Discussion

A number of epidemiological studies have shown that preeclampsia can reduce the risk of BC through different pathways (29-32). However, the specific underlying mechanism is not yet clear. This is the first study in which multi-omics

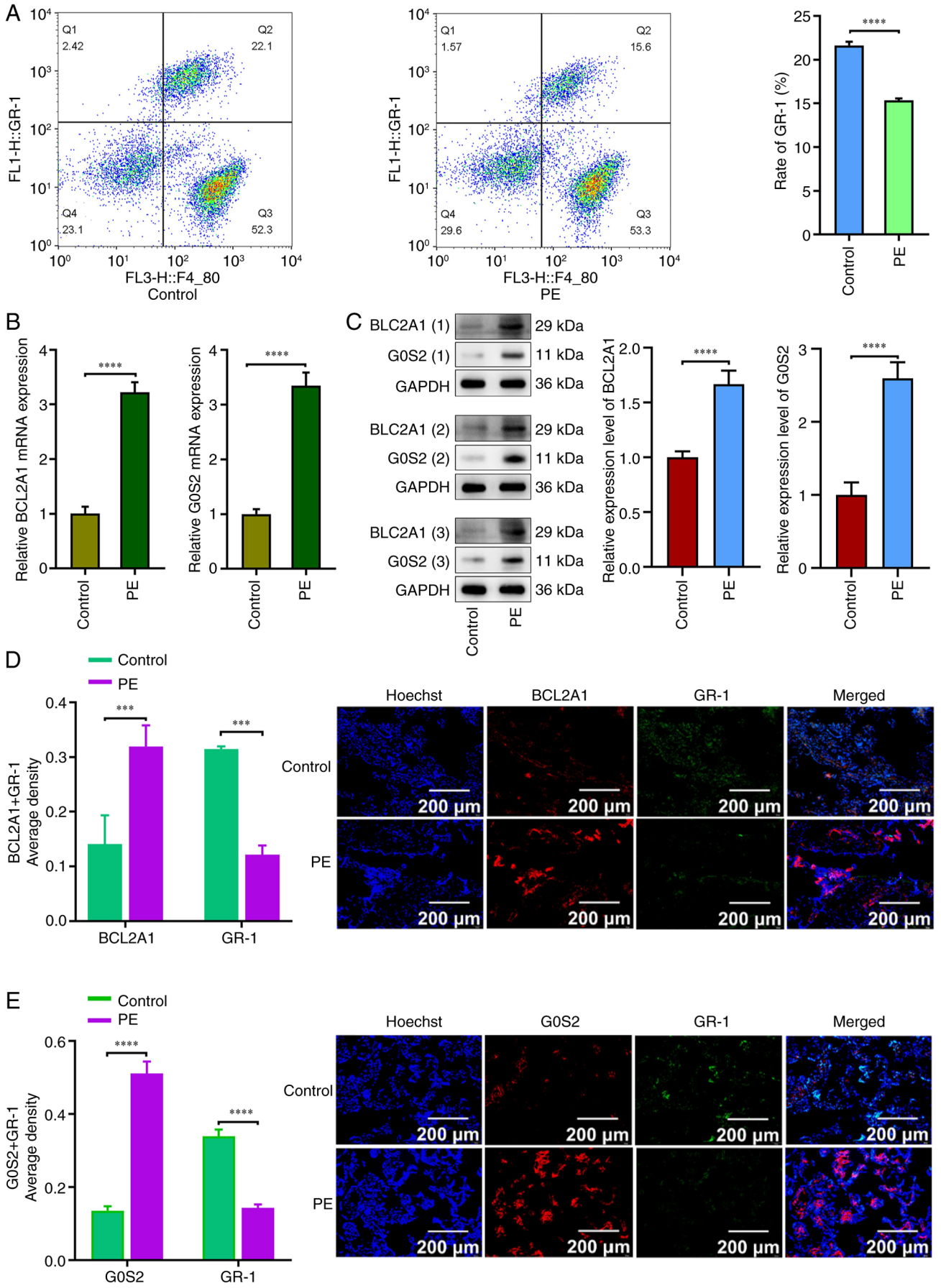

Figure 5. BCL2A1 and G0S2 genes are significantly increased in neutrophils from preeclamptic placental tissue. (A) FACS analysis showing neutrophil detection in control and preeclampsia placentas. (B and C) The mRNA and protein expression level of BCL2A1 and G0S2 in placentas. (D and E) Expression and localization of neutrophils, and BCL2A1 and G0S2 in placental tissue at x10 magnification. ***P<0.001 and ****P<0.0001. All experiments were conducted in triplicate. G0S2, G0/G1 switch gene 2; PE, preeclampsia.

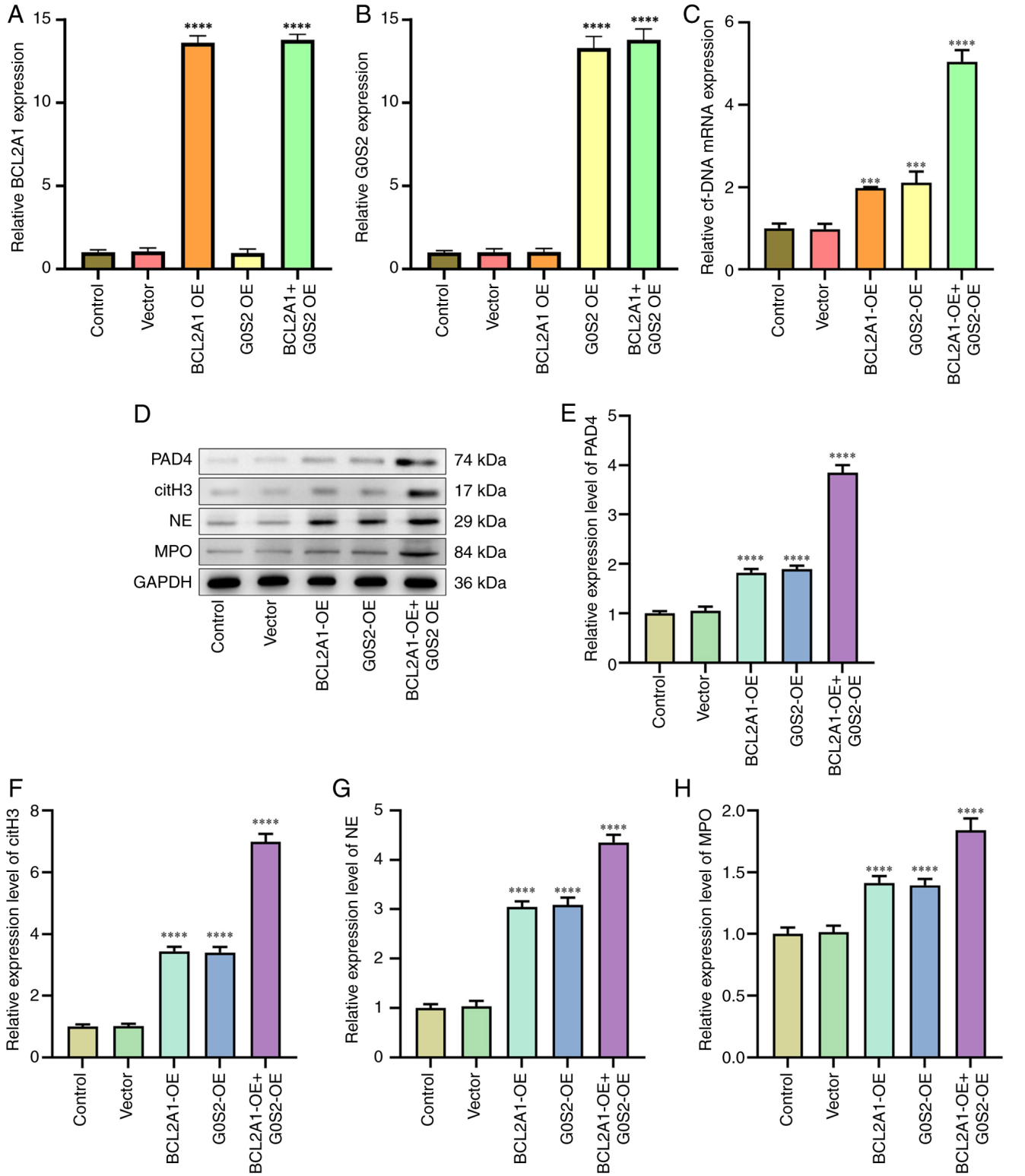

Figure 6. BCL2A1 and G0S2 genes regulate generation of neutrophil extracellular traps. (A-C) The mRNA expression level of (A) BCL2A1, (B) G0S2 and (C) cf-DNA in neutrophils upon individual and combined overexpression of BCL2A1 and G0S2. (D-H) The protein expression level of PAD4, citH3, NE and MPO in neutrophils. All comparisons were made with empty vector transfection group. ***P<0.001 and ****P<0.0001. All experiments were conducted in triplicate. MPO, myeloperoxidase; OE-, overexpressing; G0S2, G0/G1 switch gene 2.

analysis, clinical validation and cell culture experiments have been combined to reveal the specific mechanisms by which preeclampsia affects the incidence of BC. First, single-cell sequencing data provided a clear understanding of the cell-type-specific transcriptome alterations that occur in preeclampsia placental tissue. The biological processes of 27,724 cells, including trophoblasts and neutrophils, were identified in 12 different cell types. These findings indicate that the biological activities of these cells are mostly related to the cell cycle, cell migration, angiogenesis, hormone

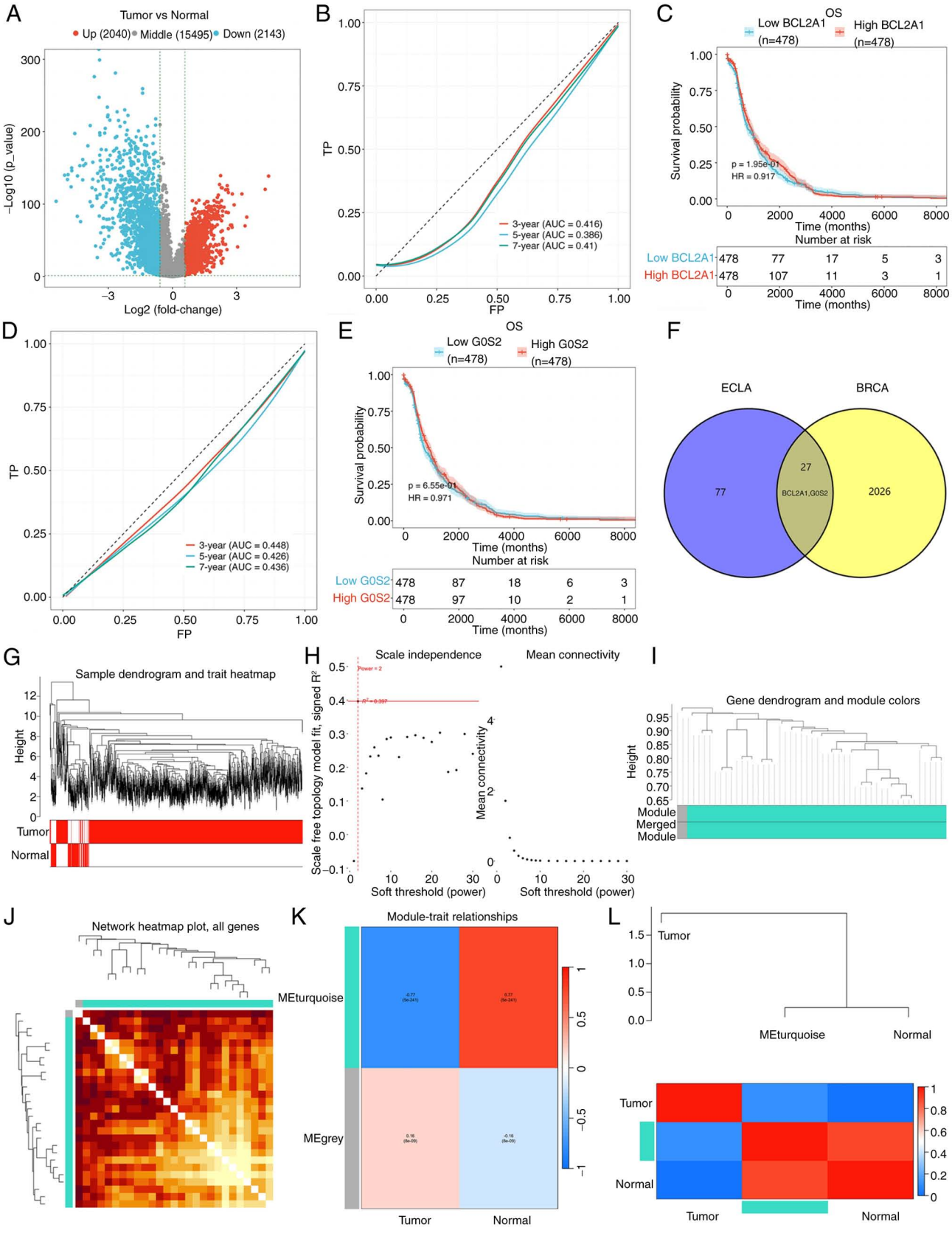

Figure 7. Clinical relationship between breast cancer and preeclampsia based on BCL2A1 and G0S2. (A) The volcano plot of DEGs in the integrated Gene Expression Omnibus (GSE24129) and TCGA-breast cancer dataset. Blue dots represent down-rgulated genes, gray dots represent not significant genes, and red dots represent upregulated genes. Blue dots indicate downregulated genes, gray dots represent genes that are not significant, and red dots signify upregulated genes. (B-E) The results of survival analysis showing that SCL2A1 and G0S2 expression levels had no obvious effect on OS. (F) Wenn diagram showing overlap of preeclampsia-associated gene from GSE24129 and genes upregulated in breast cancer from TCGA. (G-L) Weighted gene co-expression network analysis of identified DEGs. (G) A clustering dendrogram. (H) The determination of soft threshold. (I) Different modules are produced and shown in different colors by aggregating genes with strong correlations into a same module. Turquoise modules make up a greater proportion. (J) Heatmap of eigengene adjacency. (K) Clustering of modules. The turquoise module had the highest correlation with the tumor. (L) Module eigengene dendrogram. DEGs, differentially expressed genes; TCGA, The Cancer Genome Atlas; OS, overall survival; G0S2, G0/G1 switch gene 2.

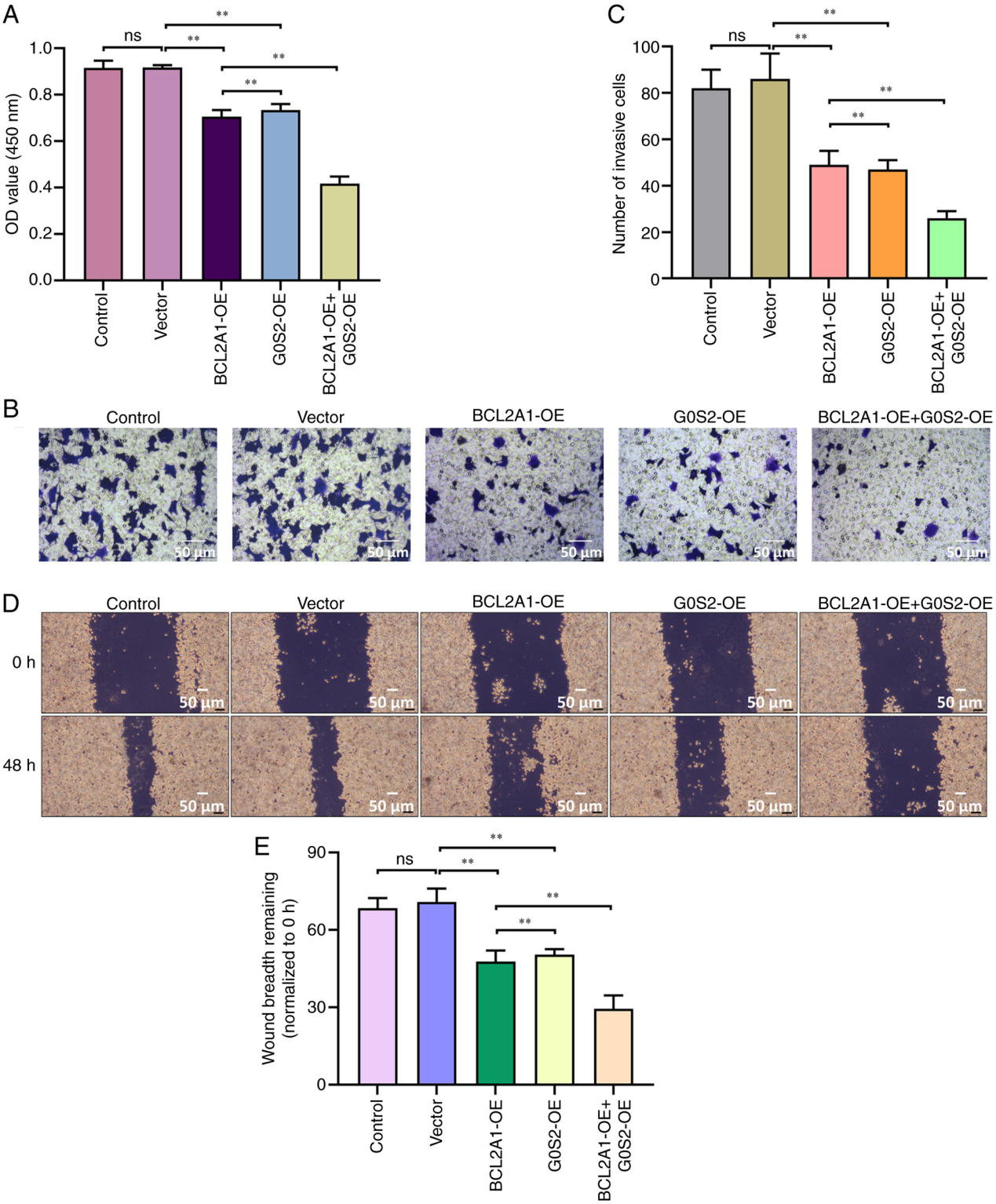

Figure 8. Overexpression of the BCL2A1 and G0S2 genes in neutrophils inhibits malignant progression of breast cancer cells. (A) Bar-graph showing changes in viability of MCF-7 cells when co-cultured with neutrophils transfected with individual or combination of BCL2A1 and G0S2 overexpression constructs. (B) Transwell assays showing the migration of MCF-7 cells at 4 magnification upon co-culturing with neutrophils transfected with individual or combination of BCL2A1 and G0S2 overexpression constructs. (C) Bar-graph showing quantification of migratory cells from (B). (D) *In vitro* scratch assay showing the migration of MCF-7 cells at x4 magnification upon co-culturing with neutrophils transfected with individual or combination of BCL2A1 and G0S2 overexpression constructs. (E) Bar-graph showing quantification of wound breadth from (D). **P<0.01. All experiments were conducted in triplicate. OE-, overexpressing; ns, not significant; G0S2, G0/G1 switch gene 2.

release and the inflammatory response. This stage of disease progression is crucial to our understanding of this disease. Therefore, the authors focused on the genes whose expression increased in neutrophils, BCL2A1 and G0S2, to further investigate the relationship between preeclampsia and BC.

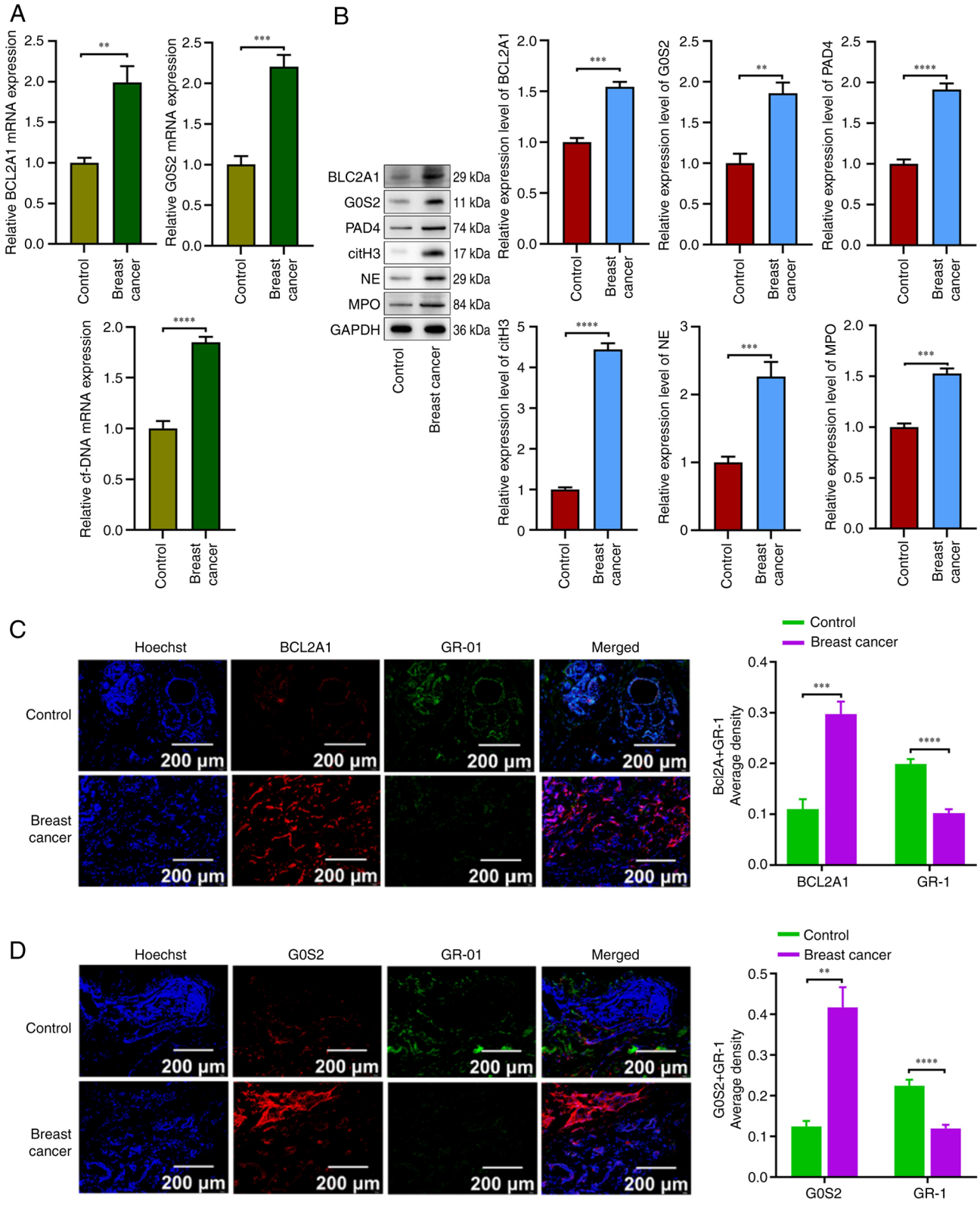

Figure 9. BCL2A1 and G0S2 gene expression levels were significantly elevated in neutrophils from breast cancer tissue, along with increase in production of neutrophil extracellular traps. (A) The mRNA expression level of BCL2A1, G0S2 and cf-DNA in breast cancer tissue compared with control. (B) The protein expression level of BCL2A1, G0S2, PAD4, citH3, NE and MPO in breast cancer tissue compared with control. (C and D) Expression and localization of neutrophils, and BCL2A1 and G0S2 in breast cancer cells at x10 magnification. **P<0.01, ***P<0.001 and ****P<0.0001. All experiments were conducted in triplicate. MPO, myeloperoxidase; G0S2, G0/G1 switch gene 2.

Based on information in the TCGA database, the associations between the differential mRNA expression in BC, patients and the BCL2A1 and G0S2 genes, and the survival rate of patients with BC were examined. Similarly, the expression of the BCL2A1 and G0S2 genes was elevated in BC. The genes upregulated in BC from the TCGA database

were combined with the preeclampsia dataset from the GEO database by Venn diagram analysis to identify 27 overlapping genes, including BCL2A1 and G0S2, to study the relationship between preeclampsia and BC. According to our findings, the BCL2A1 and G0S2 genes are associated with both preeclampsia and BC, and they may be crucial in the onset and progression of these two diseases. Using WGCNA analysis, it was also discovered that BCL2A1 and G0S2 were both important genes. As a result, BCL2A1 and G0S2 may be crucial in the disorders preeclampsia and BC.

Like other Bcl-2 family members, BCL2A1 is crucial for controlling apoptosis. It has been revealed that BCL2A1 also plays additional critical roles in vascular endothelial cells. In activated endothelial cells, TNF-α was found to be a gene caused by cytokine treatment (33). Preeclampsia is a significant pregnancy complication characterized by hypertension, proteinuria, endothelial dysfunction and an immune-inflammatory response (1). In the present study, it was discovered that neutrophils from the placental tissue of preeclampsia patients had considerably greater BCL2A1 expression. BCL2A1 is specifically involved in the pathogenesis of preeclampsia. BCL2A1 is a tightly regulated target gene of nuclear factor κB (NF-κB) that plays a crucial role in cell survival (34). Additionally, BCL2A1 is primarily expressed in the hematopoietic system, where it enhances the survival and inflammatory responses of specific subsets of leukocytes. According to previous studies, BCL2A1 is overexpressed in various cancer types, including ovarian cancer (35), BC (36), colon cancer (37) and prostate cancer (38). Furthermore, as an NF-κB target gene, BCL2A1 also plays a significant role in inflammation (34). Inflammation is a key aspect of the innate immune response, with NOD-like receptors participating in inflammasome formation under the influence of pattern recognition receptors (PRRs). One of the primary signaling pathways activated by PRRs involves the activation of NF-κB and the upregulation of proinflammatory genes (39). Consequently, the formation of inflammasomes may also trigger the expression of BCL2A1, thereby supporting the survival of proinflammatory cells during the immune response (34). The present findings suggest that the overexpression of BCL2A1 in neutrophils could promote apoptosis and inhibit the proliferation of BC cells, providing a plausible explanation for this observation.

G0S2 was initially discovered to be involved in the transition of the cell cycle from the G0 to the G1 phase induced by lectin (40). The G0S2 gene plays an important role in cell cycle regulation and apoptosis (41). Studies have shown that G0S2 can affect cell apoptosis and survival by inhibiting lipolysis and fatty acid oxidation under certain conditions (42,43). Furthermore, the expression of G0S2 may be associated with the function of vascular endothelial cells and vascular pathology. For example, G0S2 can ameliorate oxidative low-density lipoprotein-induced vascular endothelial cell damage by regulating mitochondrial apoptosis (44). Placental abnormalities and metabolic disorders are important features of preeclampsia, and adipose metabolism plays a role in these conditions (45). Moreover, adipose tissue also plays an important regulatory role in the progression of breast tumors, as adipose tissue can provide nutrients and adipokines for proliferating tumor cells. Studies have shown that fatty acid metabolism also plays an important role in various aspects of tumor cell proliferation, transformation and migration (46). It has been reported that siRNA-mediated knockdown of G0S2 leads to reduced proliferation, migration and invasion of BC cells, suggesting that G0S2 is a major factor that promotes the survival and metastasis of BC cells (47). Notably, the present findings revealed that the overexpression of G0S2 in neutrophils can reduce the proliferation, invasion and migration capacity of BC cells. This suggests that the invasion and migration of BC cells are influenced by fatty acid metabolism, where the overexpression of G0S2 can inhibit fatty acid oxidation, thereby disrupting the invasive and migratory abilities of BC cells.

Furthermore, G0S2 can localize to the endoplasmic reticulum and mitochondria (48,49). G0S2 can interact with Bcl-2, preventing the formation of the Bcl-2/Bax heterodimeric complex by controlling mitochondrial membrane permeability and cytochrome release, thereby modulating its antiapoptotic activity in human cancer cells (49). Thus, these results suggest that the synergistic effect of BCL2A1 and G0S2 in neutrophils can inhibit the growth and metastasis of BC cells.

Neutrophils are the first line of defense in the immune system, and they function by phagocytosis and degranulation. Recent research has unveiled the existence of a distinctive variant of neutrophil death, known as neutrophil necrosis. This process actively contributes to the extermination of pathogens through the extracellular release of NETs (50). NETs are intricate DNA networks filled with antimicrobial peptides that are diligently discharged by neutrophils in response to diverse stimuli. NETs are not only essential for neutrophil innate immune responses but also play a role in autoimmune diseases such as systemic lupus erythematosus, rheumatoid arthritis (51) and psoriasis (52). Additionally, they are implicated in non-infectious conditions, including coagulopathies (53), thrombosis (54), diabetes (55) and atherosclerosis (56). Notably, NETs play dual roles in tumors, serving both as facilitators and inhibitors of tumor progression. NETs composed of myeloperoxidase, proteases and histones can eliminate tumors, and impede tumor proliferation and metastasis. However, they also have the potential to degrade the extracellular matrix, promoting the escape and metastasis of cancer cells (57). In the present study, an increase was observed in the release of NETs in BC. *In vitro* cell experiments indicated that the BCL2A1 and G0S2 genes regulate the generation of NETs, leading to the inhibition of proliferation, migration and invasion in BC cells. Consequently, NETs can potentially impede the malignant progression of BC by suppressing the biological functions of these cells.

The present study has several limitations. First, the small public dataset used could skew the outcomes of the investigation. Second, the present study confirmed a lower risk of BC in preeclamptic women, which is consistent with the results reported in the majority of related studies (29-32); however, there are also conflicting results. A positive correlation was reported in one study (58), and it was also reported in two additional studies (59,60). Finally, additional research is still needed to confirm the co-expression of BCL2A1 and G0S2 as a reliable indicator of preeclampsia and BC. In conclusion, the present study proposed that neutrophils may be co-pathogenic

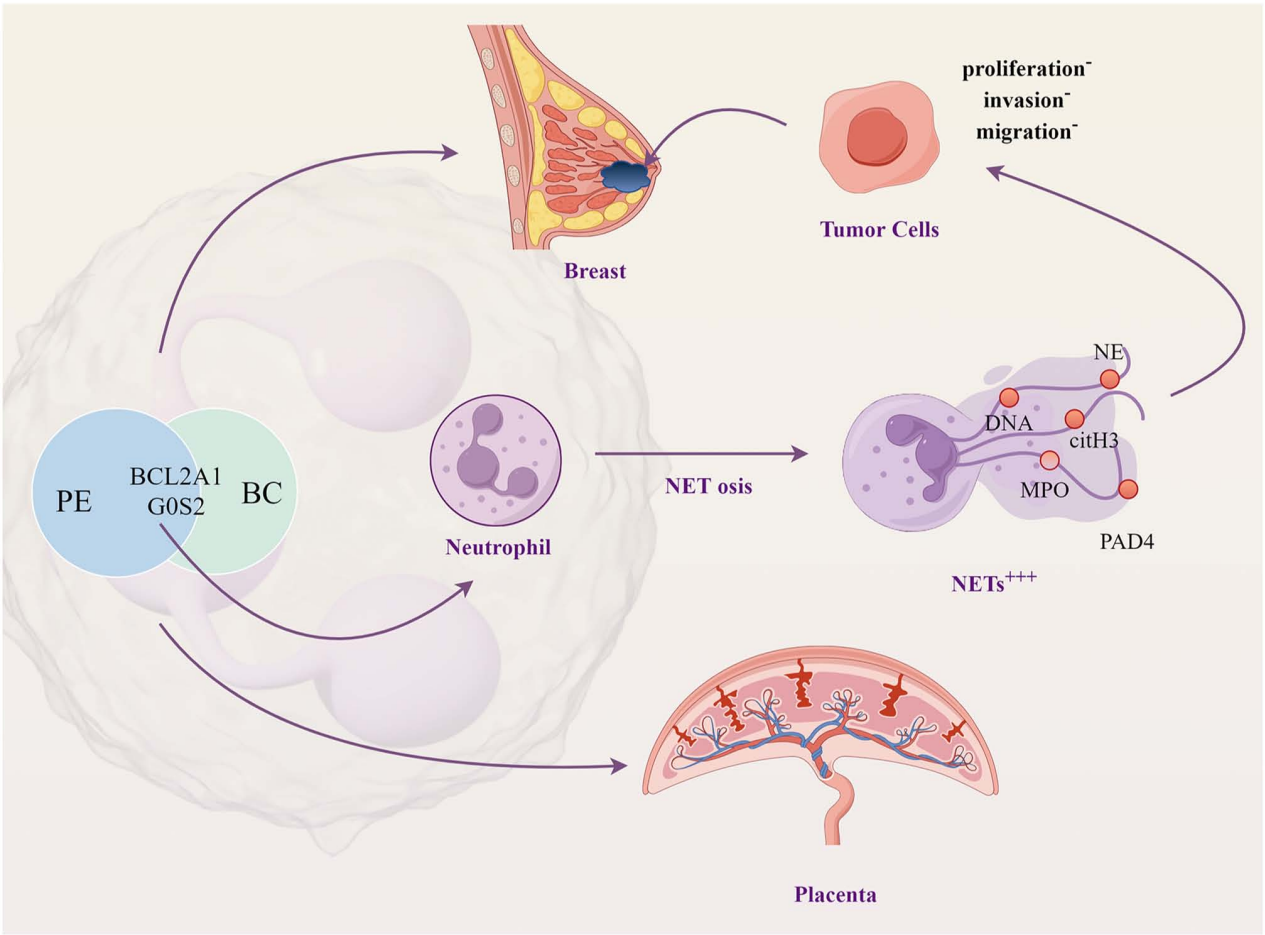

Figure 10. Mechanistic summary. The shared genes of PE and BC regulate neutrophil fate and differentiation, and then participate in promoting the release of NETs, resulting in the decreased proliferation, invasion and migratory capacity of BC cells. PE, preeclampsia; BC, breast cancer; NETs, neutrophil extracellular traps; NETosis, neutrophil necrosis.

factors between preeclampsia and BC, and further elucidated that BC risk was reduced in patients with preeclampsia due to the regulatory role of the BCL2A1 and G0S2 genes in neutrophil-mediated NET production (Fig. 10).

Acknowledgements

Not applicable.

Funding

The present study was supported by the Guangxi Natural Science Foundation Program (grant nos. 2023GXNSFAA026037 and 2024GXNSFAA010368), the Guangxi medical and health appropriate technology development and application project (grant nos. S2022080 and S2022062), the Excellent medical talents training program of the First Affiliated Hospital of Guangxi Medical University and the Project on Enhancement of Basic Research Ability of Young and Middle-aged Teachers in Guangxi Universities and Colleges (grant no. 2024KY0110).

Availability of data and materials

The data generated in the present study may be requested from the corresponding author.

Authors' contributions

LX and JinL performed data analysis and prepared figures. LX, JinL, JiaL, MW and XL performed experiments. LX wrote the manuscript. JieL and YZ designed and supervised the study, and revised the manuscript. LX and JL confirm the authenticity of all the raw data. All authors read and approved the final version of the manuscript.

Ethics approval and consent to participate

Written informed consent was obtained from all study participants for the use of tissue samples in scientific research. The present study was conducted in accordance with the ethical guidelines and was approved (approval no. 2022-E0118) by the Ethical Review Committee of the First Affiliated Hospital of Guangxi Medical University (Nanning, China).

Patient consent for publication

Not applicable.

Competing interests

The authors declare that they have no competing interests.

References

1. Rana S, Lemoine E, Granger JP and Karumanchi SA: Preeclampsia: Pathophysiology, challenges, and perspectives. Circ Res 124: 1094-1112, 2019.
2. El-Sayed AAF: Preeclampsia: A review of the pathogenesis and possible management strategies based on its pathophysiological derangements. Taiwan J Obstet Gynecol 56: 593-598, 2017.
3. Piani F, Agnoletti D, Baracchi A, Scarduelli S, Verde C, Tossetta G, Montaguti E, Simonazzi G, Degli Esposti D and Borghi C; HDP Bologna Study Group: Serum uric acid to creatinine ratio and risk of preeclampsia and adverse pregnancy outcomes. J Hypertens 41: 1333-1338, 2023.
4. Dimitriadis E, Rolnik DL, Zhou W, Estrada-Gutierrez G, Koga K, Francisco RPV, Whitehead C, Hyett J, da Silva Costa F, Nicolaides K and Menkhorst E: Pre-eclampsia. Nat Rev Dis Primers 9: 8, 2023.
5. Tossetta G, Fantone S, Giannubilo SR, Marinelli Busilacchi E, Ciavattini A, Castellucci M, Di Simone N, Mattioli-Belmonte M and Marzioni D: Pre-eclampsia onset and SPARC: A possible involvement in placenta development. J Cell Physiol 234: 6091-6098, 2019.
6. Licini C, Avellini C, Picchiassi E, Mensà E, Fantone S, Ramini D, Tersigni C, Tossetta G, Castellucci C and Tarquini F: Pre-eclampsia predictive ability of maternal miR-125b: A clinical and experimental study. Transl Res 228: 13-27, 2021.
7. Inversetti A, Pivato CA, Cristodoro M, Latini AC, Condorelli G and Di Simone N: Update on long-term cardiovascular risk after pre-eclampsia: A systematic review and meta-analysis. Eur Heart J Qual Care Clin Outcomes 10: 4-13, 2024.
8. Sung H, Ferlay J, Siegel RL, Laversanne M, Soerjomataram I, Jemal A and Bray F: Global cancer statistics 2020: GLOBOCAN estimates of incidence and mortality worldwide for 36 cancers in 185 countries. CA Cancer J Clin 71: 209-249, 2021.
9. Gilbert JS, Bauer AJ, Gilbert SA and Banek CT: The opposing roles of anti-angiogenic factors in cancer and preeclampsia. Front Biosci (Elite Ed) 4: 2652-2669, 2012.
10. Miller D, Motomura K, Galaz J, Gershater M, Lee ED, Romero R and Gomez-Lopez N: Cellular immune responses in the pathophysiology of preeclampsia. J Leukoc Biol 111: 237-260, 2022.
11. Sreeramkumar V, Adrover JM, Ballesteros I, Cuartero MI, Rossaint J, Bilbao I, Nácher M, Pitaval C, Radovanovic I, Fukui Y, *et al*: Neutrophils scan for activated platelets to initiate inflammation. Science 346: 1234-1238, 2014.
12. Chawla N, Shah H, Huynh K, Braun A, Wollocko H and Shah NC: The role of Platelet-activating factor and magnesium in obstetrics and gynecology: Is there crosstalk between pre-Eclampsia, clinical hypertension, and HELLP syndrome? Biomedicines 11: 1343, 2023.
13. Gupta AK, Hasler P, Holzgreve W and Hahn S: Neutrophil NETs: A novel contributor to Preeclampsia-associated placental hypoxia? Semin Immunopathol 29: 163-167, 2007.
14. McFarlane AJ, Fercoq F, Coffelt SB and Carlin LM: Neutrophil dynamics in the tumor microenvironment. J Clin Invest 131: e143759, 2021.
15. Li MO, Wolf N, Raulet DH, Akkari L, Pittet MJ, Rodriguez PC, Kaplan RN, Munitz A, Zhang Z, Cheng S and Bhardwaj N: Innate immune cells in the tumor microenvironment. Cancer Cell 39: 725-729, 2021.
16. Fridlender ZG, Sun J, Kim S, Kapoor V, Cheng G, Ling L, Worthen GS and Albelda SM: Polarization of tumor-associated neutrophil phenotype by TGF-beta: 'N1' versus 'N2' TAN. Cancer Cell 16: 183-194, 2009.
17. Granot Z, Henke E, Comen EA, King TA, Norton L and Benezra R: Tumor entrained neutrophils inhibit seeding in the premetastatic lung. Cancer Cell 20: 300-314, 2011.
18. Giese MA, Hind LE and Huttenlocher A: Neutrophil plasticity in the tumor microenvironment. Blood 133: 2159-2167, 2019.
19. Hirschhorn D, Budhu S, Kraehenbuehl L, Gigoux M, Schröder D, Chow A, Ricca JM, Gasmi B, De Henau O, Mangarin LMB, *et al*: T cell immunotherapies engage neutrophils to eliminate tumor antigen escape variants. Cell 186: 1432-1447.e17, 2023.
20. Lun ATL, Riesenfeld S, Andrews T, Dao TP and Gomes T; participants in the 1st Human Cell Atlas Jamboree; Marioni JC: EmptyDrops: Distinguishing cells from empty droplets in Droplet-based Single-cell RNA sequencing data. Genome Biol 20: 63, 2019.
21. McCarthy DJ, Campbell KR, Lun AT and Wills QF: Scater: Pre-processing, quality control, normalization and visualization of single-cell RNA-seq data in R. Bioinformatics 33: 1179-1186, 2017.
22. Hao Y, Hao S, Andersen-Nissen E, Mauck WM III, Zheng S, Butler A, Lee MJ, Wilk AJ, Darby C, Zager M, *et al*: Integrated analysis of multimodal single-cell data. Cell 184: 3573-3587.e29, 2021.
23. Puthumana J, Thiessen-Philbrook H, Xu L, Coca SG, Garg AX, Himmelfarb J, Bhatraju PK, Ikizler TA, Siew ED, Ware LB, *et al*: Biomarkers of inflammation and repair in kidney disease progression. J Clin Invest 131: e139927, 2021.
24. Jin S, Guerrero-Juarez CF, Zhang L, Chang I, Ramos R, Kuan CH, Myung P, Plikus MV and Nie Q: Inference and analysis of cell-cell communication using CellChat. Nat Commun 12: 1088, 2021.
25. Trapnell C, Cacchiarelli D, Grimsby J, Pokharel P, Li S, Morse M, Lennon NJ, Livak KJ, Mikkelsen TS and Rinn JL: The dynamics and regulators of cell fate decisions are revealed by pseudotemporal ordering of single cells. Nat Biotechnol 32: 381-386, 2014.
26. Langfelder P and Horvath S: WGCNA: An R package for weighted correlation network analysis. BMC Bioinformatics 9: 559, 2008.
27. Livak KJ and Schmittgen TD: Analysis of relative gene expression data using real-time quantitative PCR and the 2(-Delta Delta C(T)) method. Methods 25: 402-408, 2001.
28. Zhou W, Wang H, Yang Y, Guo F, Yu B and Su Z: Trophoblast cell subtypes and dysfunction in the placenta of individuals with preeclampsia revealed by SingleCell RNA sequencing. Mol Cells 45: 317-328, 2022.
29. Powell M, Fuller S, Gunderson E and Benz C: A common IGF1R gene variant predicts later life breast cancer risk in women with preeclampsia. Breast Cancer Res Treat 197: 149-159, 2023.
30. Nichols HB, House MG, Yarosh R, Mitra S, Goldberg M, Bertrand KA, Eliassen AH, Giles GG, Jones ME, Milne RL, *et al*: Hypertensive conditions of pregnancy, preterm birth, and premenopausal breast cancer risk: A premenopausal breast cancer collaborative group analysis. Breast Cancer Res Treat 199: 323-334, 2023.
31. Opdahl S, Romundstad PR, Alsaker MDK and Vatten LJ: Hypertensive diseases in pregnancy and breast cancer risk. Br J Cancer 107: 176-182, 2012.
32. Vatten LJ, Romundstad PR, Trichopoulos D and Skjaerven R: Pre-eclampsia in pregnancy and subsequent risk for breast cancer. Br J Cancer 87: 971-973, 2002.
33. Karsan A, Yee E, Kaushansky K and Harlan JM: Cloning of human Bcl-2 homologue: Inflammatory cytokines induce human A1 in cultured endothelial cells. Blood 87: 3089-3096, 1996.
34. Vogler M: BCL2A1: The underdog in the BCL2 family. Cell Death Differ 19: 67-74, 2011.
35. Liang R, Yung MMH, He F, Jiao P, Chan KKL, Ngan HYS and Chan DW: The Stress-inducible BCL2A1 is required for ovarian cancer metastatic progression in the peritoneal microenvironment. Cancers (Basel) 13: 4577, 2021.
36. Murthy SRK, Cheng X, Zhuang T, Ly L, Jones O, Basadonna G, Keidar M and Canady J: BCL2A1 regulates Canady Helios Cold Plasma-induced cell death in triple-negative breast cancer. Sci Rep 12: 4038, 2022.
37. Yue T, Liu X, Zuo S, Zhu J, Li J, Liu Y, Chen S and Wang P: BCL2A1 and CCL18 are predictive biomarkers of cisplatin chemotherapy and immunotherapy in colon cancer patients. Front Cell Dev Biol 9: 799278, 2021.
38. Pucci P, Venalainen E, Alborelli I, Quagliata L, Hawkes C, Mather R, Romero I, Rigas SH, Wang Y and Crea F: LncRNA HORAS5 promotes taxane resistance in castration-resistant prostate cancer via a BCL2A1-dependent mechanism. Epigenomics 12: 1123-1138, 2020.
39. Takeuchi O and Akira S: Pattern recognition receptors and inflammation. Cell 140: 805-820, 2010.
40. Russell L and Forsdyke DR: A human putative lymphocyte G0/G1 switch gene containing a CpG-rich island encodes a small basic protein with the potential to be phosphorylated. DNA Cell Biol 10: 581-591, 1991.
41. Heckmann BL, Zhang X, Xie X and Liu J: The G0/G1 switch gene 2 (G0S2): Regulating metabolism and beyond. Biochim Biophys Acta 1831: 276-281, 2013.
42. Zhang X, Heckmann BL, Campbell LE and Liu J: G0S2: A small giant controller of lipolysis and adipose-liver fatty acid flux. Biochim Biophys Acta Mol Cell Biol Lipids 1862: 1146-1154, 2017.

43. Yang X, Lu X, Lombès M, Yang X, Lu X and Lombès M: The G(0)/G(1) switch gene 2 regulates adipose lipolysis through association with adipose triglyceride lipase. Cell Metab 11: 194-205, 2010.
44. Liang Z, Diao W, Jiang Y and Zhang Y: G0S2 ameliorates oxidized low-density lipoprotein-induced vascular endothelial cell injury by regulating mitochondrial apoptosis. Ann Transl Med 10: 1383, 2022.
45. Kaaja R, Tikkanen MJ, Viinikka L and Ylikorkala O: Serum lipoproteins, insulin, and urinary prostanoid metabolites in normal and hypertensive pregnant women. Obstet Gynecol 85: 353-356, 1995.
46. Wu X, Deng F, Li Y, Daniels G, Du X, Ren Q, Wang J, Wang LH, Yang Y, Zhang V, *et al*: ACSL4 promotes prostate cancer growth, invasion and hormonal resistance. Oncotarget 6: 44849-44863, 2015.
47. Cho E, Kwon YJ, Ye DJ, Baek HS, Kwon TU, Choi HK and Chun YJ: G0/G1 switch 2 induces cell survival and metastasis through Integrin-mediated signal transduction in human invasive breast cancer cells. Biomol Ther (Seoul) 27: 591-602, 2019.
48. Zandbergen F, Mandard S, Escher P, Tan NS, Patsouris D, Jatkoe T, Rojas-Caro S, Madore S, Wahli W, Tafuri S, *et al*: The G0/G1 switch gene 2 is a novel PPAR target gene. Biochem J 392: 313-324, 2005.
49. Welch C, Santra MK, El-Assaad W, Zhu X, Huber WE, Keys RA, Teodoro JG and Green MR: Identification of a protein, G0S2, that lacks Bcl-2 homology domains and interacts with and antagonizes Bcl-2. Cancer Res 69: 6782-6789, 2009.
50. Islam MM and Takeyama N: Role of neutrophil extracellular traps in health and disease pathophysiology: Recent insights and advances. Int J Mol Sci 24: 15805, 2023.
51. Fresneda Alarcon M, McLaren Z and Wright HL: Neutrophils in the pathogenesis of rheumatoid arthritis and systemic lupus erythematosus: Same Foe Different M.O. Front Immunol 12: 649693, 2021.
52. Shao S, Fang H, Dang E, Xue K, Zhang J, Li B, Qiao H, Cao T, Zhuang Y, Shen S, *et al*: Neutrophil extracellular traps promote inflammatory responses in psoriasis via activating epidermal TLR4/IL-36R crosstalk. Front Immunol 10: 746, 2019.
53. Jin J, Wang F, Tian J, Zhao X, Dong J, Wang N, Liu Z, Zhao H, Li W, Mang G and Hu S: Neutrophil extracellular traps contribute to coagulopathy after traumatic brain injury. JCI Insight 8: e141110, 2023.
54. Van Bruggen S and Martinod K: The coming of age of neutrophil extracellular traps in thrombosis: Where are we now and where are we headed? Immunol Rev 314: 376-398, 2022.
55. Yang S, Wang S, Chen L, Wang Z, Chen J, Ni Q, Guo X, Zhang L and Xue G: Neutrophil extracellular traps delay diabetic wound healing by inducing Endothelial-to-Mesenchymal transition via the hippo pathway. Int J Biol Sci 19: 347-361, 2023.
56. Sano M, Maejima Y, Nakagama S, Shiheido-Watanabe Y, Tamura N, Hirao K, Isobe M and Sasano T: Neutrophil extracellular traps-mediated Beclin-1 suppression aggravates atherosclerosis by inhibiting macrophage autophagy. Front Cell Deve Biol 10: 876147, 2022.
57. Masucci MT, Minopoli M, Del Vecchio S and Carriero MV: The emerging role of neutrophil extracellular traps (NETs) in tumor progression and metastasis. Front Immunol 11: 1749, 2020.
58. Calderon-Margalit R, Friedlander Y, Yanetz R, Deutsch L, Perrin MC, Kleinhaus K, Tiram E, Harlap S and Paltiel O: Preeclampsia and subsequent risk of cancer: Update from the Jerusalem Perinatal Study. Am J Obstet Gynecol 200: 63.e1-5, 2009.
59. Brasky TM, Li Y, Jaworowicz DJ Jr, Potischman N, Ambrosone CB, Hutson AD, Nie J, Shields PG, Trevisan M, Rudra CB, *et al*: Pregnancy-related characteristics and breast cancer risk. Cancer Causes Control 24: 1675-1685, 2013.
60. Nechuta S, Paneth N and Velie EM: Pregnancy characteristics and maternal breast cancer risk: A review of the epidemiologic literature. Cancer Causes Control 21: 967-989, 2010.